



Excess Conductivity and Critical Physical Parameters of Y Substituted Ca Site of Bi: 2223 High T_c Superconductors

A. Sedky^{1*}, Amna Salah¹ and S. A. Amin¹

¹*Department of Physics, Faculty of Science, Assiut University, Assiut, Egypt.*

Authors' contributions

This work was carried out in collaboration between all authors. All authors are participating together in suggesting the problem, data fitting and plotting, analysis and interpretation the results, writing article, preparing the submitted and revised article forms. Finally, all authors read and approved the final manuscript.

Article Information

DOI: 10.9734/AJOPACS/2017/36244

Editor(s):

(1) Dung Dinh Luong, Tandon School of Engineering, Department of Mechanical and Aerospace Engineering, New York University, New York.

Reviewers:

(1) Yong Gan, California State Polytechnic University, USA.

(2) Mehmet Çavaş, Firat University, Turkey.

Complete Peer review History: <http://www.sciencedomain.org/review-history/21326>

Original Research Article

Received 19th August 2017
Accepted 6th September 2017
Published 11th October 2017

ABSTRACT

We presented here the fluctuation induced excess conductivity in $\text{Bi}_{1.7}\text{Pb}_{0.3}\text{Sr}_2\text{Ca}_{2-x}\text{Y}_x\text{Cu}_3\text{O}_y$ superconductors with various x values ($0.00 \leq x \leq 0.50$). The logarithmic plots of excess conductivity ($\Delta\sigma$) and reduced temperature (ε) reveal three different values of the order parameter dimensional exponents against a decrease of temperature corresponding to two different values of crossover temperatures. In the critical field region, the order parameter exponents are two dimensional (2D) as x increases up to 0.20, but it is changed to three dimensional (3D) with further increase of x up to 0.50. While, the order parameter exponents are not systematic with Y in both normal and mean field regions, and they are fluctuated between zero dimensional /short wave (0D/SW), quasi-2D, quasi-1D and 3D. On the other hand, the coherence lengths, inter-plane spacing, interlayer coupling, G-L parameter and anisotropy are calculated and their values are generally increased by increasing x up to 0.50, whereas G-L parameter, Ginsburg number, critical magnetic fields and critical current density are decreased. The possible reasons for the above findings are also mentioned.

*Corresponding author: E-mail: sedky1960@yahoo.com;

Keywords: Fluctuation; excess conductivity; critical parameters; order parameter and critical fields.

1. INTRODUCTION

The doping processes in high temperature superconductors have been used early to improve their properties in parallel with special focusing on their applications [1,2]. The Bi: 2223 superconducting system with T_c of 110 K is the most widely studied superconductor, because it differs with the other superconductors in the number of both CuO_2 planes and Ca layers [3]. Furthermore, the Bi: 2223 system has higher critical current density J_c and critical magnetic fields H_c as compared to Y: 123 systems [4,5].

The well established diagram of the high temperature superconductors against carrier concentration indicate that the systems are Mott-Hubbard insulator in the under doped region and superconductor in the intermediate range, whereas in the over doped region they are normal metal [6-7]. However, carrier concentration in the high T_c superconducting systems may be varied either by varying the doping content or oxygen deficient, leading to dramatic changes in the transport behavior, and simultaneously influence the T_c values [8,9].

Due to short coherence length and high T_c in superconductors, the thermal fluctuation of superconducting order parameter has been early observed as excess conductivity [10-11]. The fluctuation of Cooper pairs begin to be created spontaneously at a temperature higher than twice mean field temperature T_c^{mf} ($T \geq 2T_c^{mf}$), and normally increases as the temperature approaches critical temperature T_c . The mean field temperature T_c^{mf} is the temperature at which the fluctuation induced conductivity regime separates from the critical fluctuation regime, and normally obtained close to T_c [12-15]. This is simply obtained from the optimum value of the (dp/dT) against temperature plot as a simple method.

The fluctuation induced conductivity (FIC) analyses reveal that the contribution of excess conductivity is mainly due to Gaussian and critical fluctuations in the mean field and critical field regions, respectively [16]. Gaussian fluctuation is probably dominant in the temperature region above the T_c^{mf} when the fluctuation in the order parameter is small and the interactions between Cooper pairs can be neglected. While the critical fluctuation occurs in the critical field region below the T_c^{mf} when the

fluctuations in the order parameter are large and the interactions between Cooper pairs is considered.

The variation of induced excess conductivity due to Gaussian fluctuation with the reduced temperature ϵ helps for finding the dimensional exponents, coherence lengths, interlayer coupling, inter-plane spacing and crossover temperatures [17-18]. The dimensional exponents in high T_c materials are found to be zero dimensional or spin wave (0D/SW), one dimensional (1D), two dimensional (2D) and three dimensional (3D). It is seen that the dimensional crossover takes place between any two different dimensions regions, and it is mainly obtained above T_c in most of high T_c systems [19-20].

The fluctuation conductivity is an important topic because it directly examines the possibility for the electron pairs formation at a temperature above T_c . According to the one of existing concept, the pseudogap is formed above T_c due to superconducting fluctuations, and usually leads to electron pairs formation, which serves as a precursor to the transition into superconducting state. Nevertheless the fluctuation studies based on pure Bi: 2223 superconducting systems in the vicinity of T_c are well described by 2D or quasi-2D nature as a result of good interlayer coupling. It may also become 3D depending on a heat treatment that modifies the state of microscopic disorder and induces spatial fluctuations near T_c [21]. The doping of rare earth elements at Ca sites in Bi: 2223 superconductors mutually have different results based on fluctuation study of induced excess conductivity which may be alters the carrier concentration in the CuO_2 planes. The doping of Pr, Ce, Gd and Cd doped at Ca sites in Bi: 2223 system suggest 2D superconducting order parameter, and a distinct 2D-3D crossover behavior is obtained near T_c [22-27]. Furthermore, the doping at sufficiently high dopant concentrations may alter the carrier concentration in the CuO_2 planes and leads to a T_c depression and usually causes a metal-insulator transition. But these studies however, do not discuss in details the effects of Y substitution in Bi: 2223 systems on the behavior of superconducting fluctuation especially in the over doped region. Moreover, some of the physical parameters such as coherence lengths, inter-plane spacing, interlayer coupling, G-L

parameter, anisotropy, critical fields and critical current are not summarized in details. However, structural and superconducting properties of $\text{Bi}_{1.7}\text{Pb}_{0.3}\text{Sr}_2\text{Ca}_{2-x}\text{Y}_x\text{Cu}_3\text{O}_y$ superconductors with various x values are well investigated by A. Sedky [28]. Although T_c was gradually decreased by increasing x up to 0.50, it found that Y has a higher solubility in the Bi (Pb):2223 system and is less detrimental to the superconductivity as compared with the other rare earth elements R. At present, there is an ample interest for investigating the fluctuation induced conductivity of the same bath of samples and able to calculate some of superconducting physical parameters. However, it is found that Y substitution shift the order parameter exponents of Bi: 2223 in the critical field region from 2D to 3D as x increases above 0.20. Furthermore, decreasing the values of Ginsburg number and G-L parameter support the decrease of critical fields and critical current as well as T_c .

2. EXPERIMENTAL DETAILS

As reported by A.Sedky [28], $\text{Bi}_{1.7}\text{Pb}_{0.3}\text{Sr}_2\text{Ca}_{2-x}\text{Y}_x\text{Cu}_3\text{O}_y$ samples are prepared by using solid-state reaction method. $\text{Bi}_{1.7}\text{Pb}_{0.3}\text{Sr}_2\text{Ca}_{2-x}\text{Y}_x\text{Cu}_3\text{O}_y$ samples with various x values are prepared by using solid-state reaction method. The ingredients of Bi_2O_3 , PbO , SrO , Y_2O_3 , CaCO_3 and CuO of 4N purity are thoroughly mixed in required proportions and calcined at 820°C in air for 24 h. This exercise is repeated three times with intermediate grinding at each stage. The resulting powder is reground, mixed, pressed into pellets and sintered at 845°C for 150 h in air. Finally the pellets are slowly cooled to room temperature. The phase purity of the samples is examined by using X-ray diffract meter (XRD). The electrical resistivity of the samples

$\rho = \frac{RA}{\ell}$ are obtained as a function of

temperature using the standard four-probe technique in closed cycle refrigerator [cryomech compressor package with cryostat Model 810-1812212, USA] within the range of (10-300K). Nanovoltmeter Keithley 2182, current source Keithley 6220 and temperature controller 9700 (0.001 K resolution) are used in this experiment. Silver paste is used for making currents and voltage contacts. A current (1-5) mA is passing through the sample and the voltage across the sample is measured by using nanovoltmeter. The values of resistivity are obtained from the values of voltage and sample dimensions A and ℓ .

3. RESULTS AND DISCUSSION

The results of XRD patterns as reported in [28] indicated that most of high intensity peaks belong to the 2223 tetragonal phase with a few low intensity peaks belong to 2212 phase. The c -parameter is decreased with increasing x , whereas a -parameter increases. The decrease in c - parameter with Y content is due to smaller ionic size of Y^{3+} (1.02 Å) ions compared to the Ca^{2+} (1.12 Å) at the same 8-fold coordination. While, the increase in the a -parameter may result from a decrease in the hole carrier concentration per Cu ion, which weakens the Cu-O bond. The gradual depression of T_c ($p = 0.00$) from 106 K to 101, 93, 79, 55 and 21 K by Y^{3+} substitution is listed in Table 1 and shown in Fig. 2(b). This is due to increasing the hole carriers concentration per Cu ion in the superconducting state from the optimum doped region to the over doped region as x increases. In this case, more positive charges are transferred to the Cu- O_2 planes in the Bi:2223 system and helps for decreasing T_c [28-29].

The excess conductivity $\Delta\sigma$ due to thermal fluctuation is defined by the deviation of the measured conductivity of $\sigma_m(T)$ from the normal conductivity $\sigma_n(T)$ as follows;

$$\Delta\sigma = \left(\frac{1}{\rho_m} - \frac{1}{\rho_n} \right) = \sigma_m - \sigma_n \quad (1)$$

where ρ_m and ρ_n are the measured and normal resistivity, respectively. ρ_n is obtained from the measured resistivity ρ_m at $T \geq 2T_c$ by applying the least square method to the Anderson and Zou relation , $\rho_n(T) = A + BT$ [30]. $\rho_n(T)$ is calculated in terms of A and B parameters that obtained from the linear fit of the measured resistivity $\rho_m(T)$ as shown in Fig. 1(a-f).

In order to estimate the paraconductivity, Aslamazov and Larkin (AL) deduced the following relation for the fluctuation- induced excess conductivity $\Delta\sigma$ as [30];

$$\Delta\sigma = A\varepsilon^{-\lambda} \quad (2)$$

Here, $A = \frac{e^2}{32\hbar\xi_c(0)}$ for 3D, $A = \frac{e^2}{32\hbar d}$ for 2D and

$A = \frac{e^2\xi_c(0)}{32\hbar S}$ for 1D, e is the electronic charge, d

is the interlayer spacing between two successive CuO_2 planes, \hbar is the reduced Planks' constant, $\xi_c(0)$ is the c-axis 3D coherence length at zero temperature, S is the wire cross-sectional area of the 1D system, λ is an exponent related with the actual conduction dimensionality. The values of the exponent's λ are 2, 0.5, 1 and 1.5 for (0D/SW), 3D, 2D and 1D fluctuations respectively, and ε is the reduced temperature given by $\varepsilon = \frac{T - T_c^{mf}}{T_c^{mf}}$ [30-32]. Where T_c^{mf} is

the mean field temperature above it the interactions between Cooper pairs can be neglected. T_c^{mf} for all samples are estimated from the peak of $d\rho/dT$ against temperature plot as shown in Fig. 2 (a), and similar values are listed in Table 1. However, the variation of T_c and T_c^{mf} against x content is shown in Fig. 2 (b). It is clear that T_c^{mf} is decreased as x increases as well as T_c .

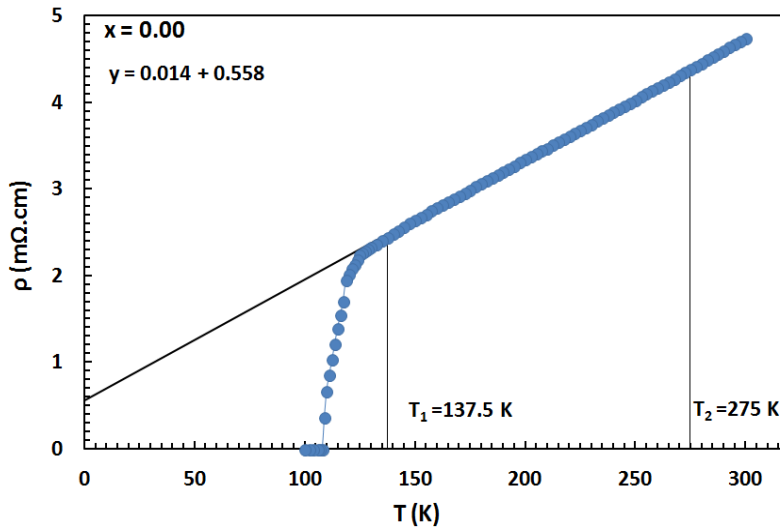


Fig. 1 (a). Resistivity versus temperature for Y doped Bi:2223 samples ($x= 0.00$)

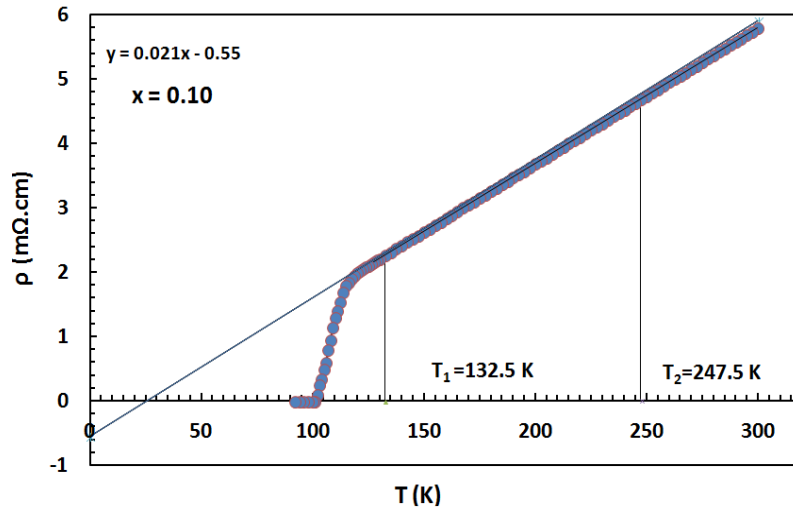


Fig. 1 (b). Resistivity versus temperature for Y doped Bi:2223 samples ($x=0.10$)

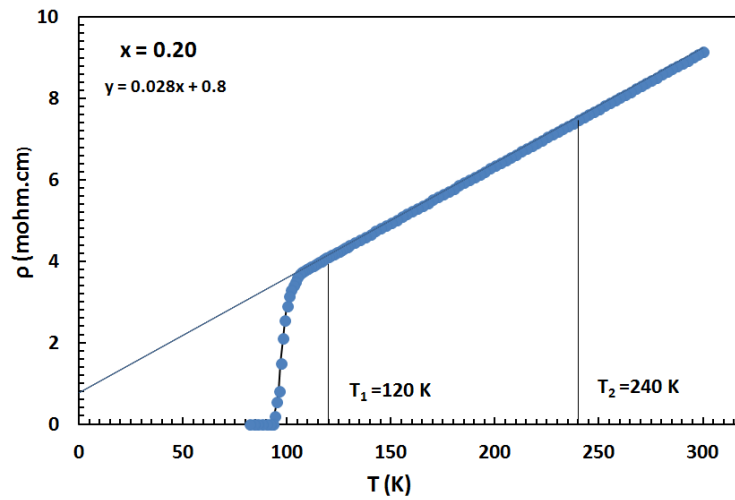


Fig. 1 (c). Resistivity versus temperature for Y doped Bi:2223 samples ($x=0.20$)

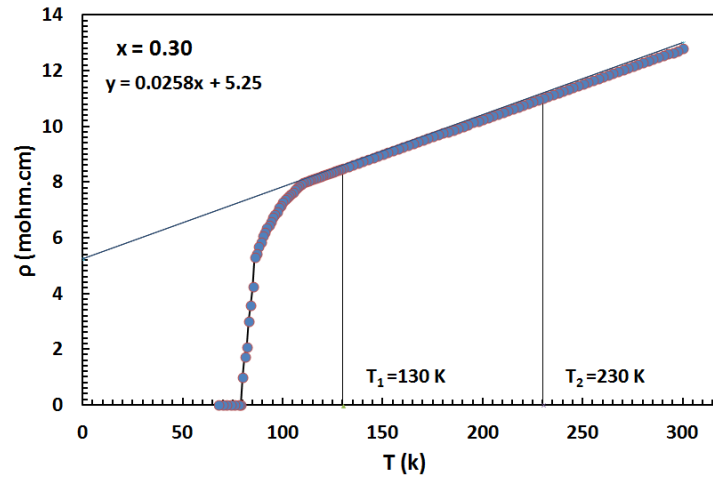


Fig. 1(d). Resistivity versus temperature for Y doped Bi:2223 samples ($x=0.30$)

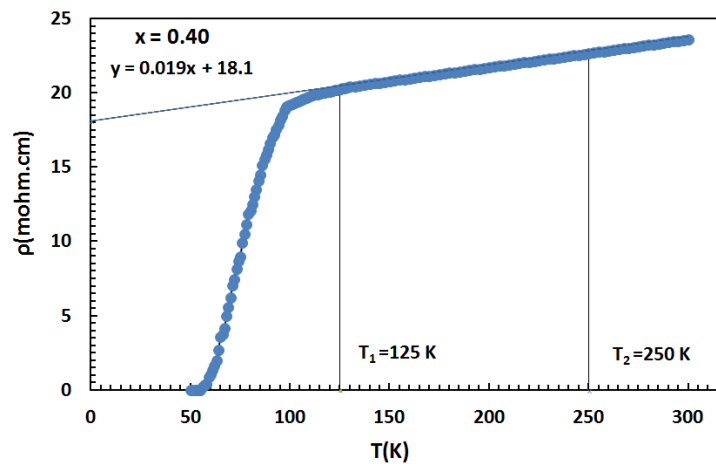


Fig. 1 (e). Resistivity versus temperature for Y doped Bi:2223 samples ($x=0.40$)

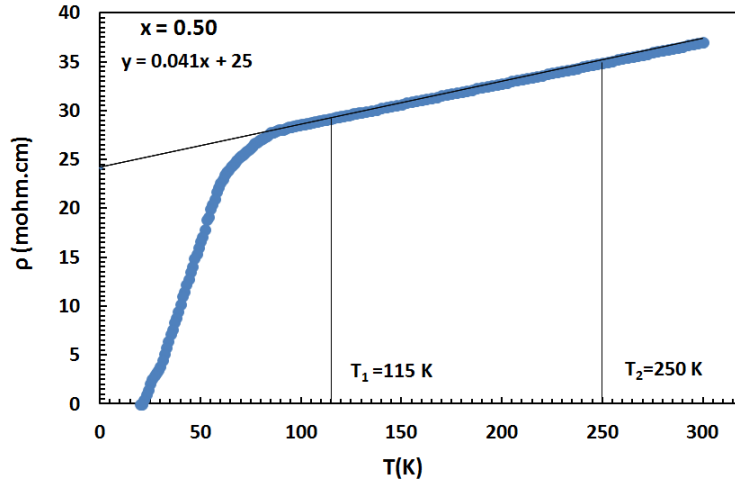


Fig. 1 (f). Resistivity versus temperature for Y doped Bi:2223 samples ($x = 0.50$)

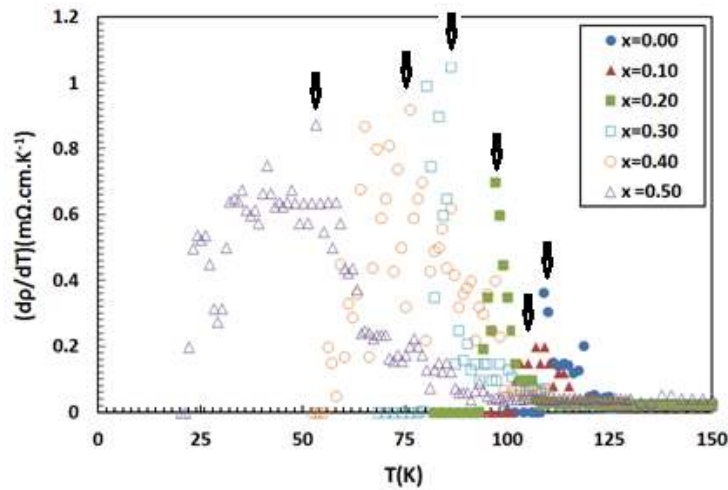


Fig. 2 (a). dp/dT versus temperature for Y doped Bi:2223 samples

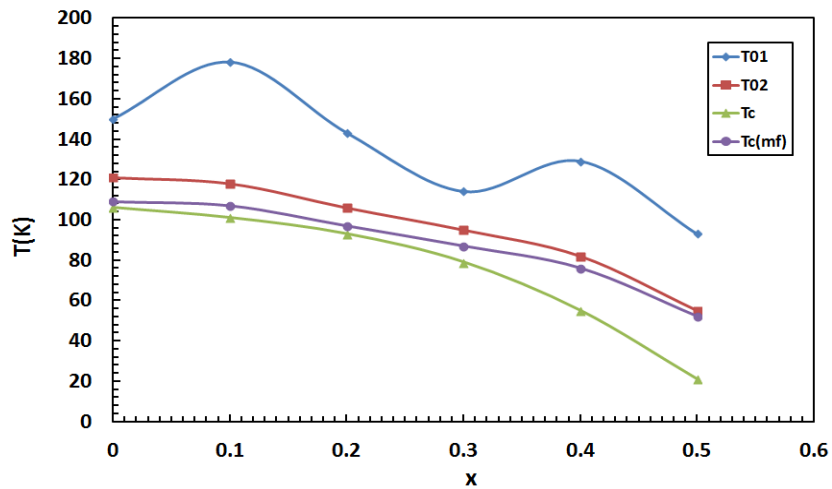


Fig. 2(b). T_c , T_c^{mf} and T_0 versus x for Y doped Bi:2223 samples

We have calculated and plotted the excess conductivity $\ln\Delta\sigma$ against reduced temperature $\ln\varepsilon$ and shown in Fig. 3(a-f). However, it is evident from the fitting that there are two distinct changes in the slope of each plot; the first is in the normal field region, while the second is in the mean field region. The corresponding temperatures where the slope change occurs are designated as the crossover temperatures T_{01} and T_{02} . The variation of crossover temperatures against x is shown in Fig. 2(b), and similar values are listed in Table 1. It is clear that T_{01} is not systematic with x content, but it is generally decreased as x increases as compared to pure sample. The higher value of T_{01} in the normal field region at $x = 0.10$ means that a sizable fraction of Y may be residing outside the superconducting grains, and helps for shifting the cross-over temperature to higher value. As x increases above 0.10, a convenient fraction of Y is residing inside the grains, and then T_{01} shifted to lower values [33]. T_{02} is gradually decreased as x increases as well as T_c and T_c^{mf} behaviors.

The crossover behavior could be explained according to the highly anisotropy of superconductor, where the charge carriers move more readily in some directions than in the others. Further, the charge carriers have ability to move along the superconducting planes in the superconductor within a range of temperature selected at which the thermal fluctuations of charge carriers exist. A crossover behavior due thermal fluctuations takes place by cooling the superconductor down to a lower temperature, and therefore the charge carriers may move between the superconducting planes and crossover from one plane to another. This means that the charge carriers tend to move more freely

in the whole sample before they make pairs in the mean field region above T_c [34-36].

Three different exponents of the order parameter dimensionality could be obtained from the slopes of each plot as shown in Fig. 3 (a-f). These values are arranged towards low temperature region as λ_I , λ_{II} and λ_{III} for $x = 0.00, 0.10, 0.20, 0.30, 0.40$ and 0.50 , respectively. The first exponents λ_I are obtained in the normal field region at a temperature range of $\ln\varepsilon$ ($0.00 \geq \ln\varepsilon \geq 1.5$), and their values are 0.59 (quasi-2D), 1.34 (quasi-1D), 0.90 (2D), 0.81 (2D), 0.15 (quasi-3D) and 0.65 (quasi-2D). The second exponents λ_{II} are obtained at the mean field region at a temperature range of $\ln\varepsilon$ ($-0.50 \geq \ln\varepsilon \geq -2.5$), and their values are 2.37 (0D/SW), 0.49 (3D), 0.34 (3D), 2.56 (0D/SW), 2.52 (0D/SW) and 1.97 (0D/SW). The third exponents λ_{III} are obtained in the mean field region at a temperature range of $\ln\varepsilon$ ($-2 \geq \ln\varepsilon \geq -4.5$) and their values are 0.91 (2D), 1.09 (2D), 1.17 (2D), 0.45 (3D), 0.46 (3D) and 0.34 (3D). The appearance (0D/SW) in these types of samples may be due to short wave length fluctuations in the considered region [26,27]. Our interesting point here is observed for the third values of exponents in the mean field region, where the order parameter is shifted from 2D to 3D as the x increases above 0.20. This is may be related to the effective length in the direction perpendicular to the current flow which is found to be more reduced in Y doped Bi:2223 as x increases up to 0.50 [37]. Further, the obtained (0D/SW) of the order parameter below T_c is due critical fluctuations in the conductivity region of microscopic granular superconductor, and it is extremely sensible to applied magnetic field [21].

Table 1. $T_c, T_c^{mf}, T_{01}, T_{02}, J, d, \xi_c(0), \lambda_I, \lambda_{II}$ and λ_{III} for Y doped Bi:2223 samples

X	T_c K	T_c^{mf} K	T_{01} K	T_{02} K	J	d (Å)	$\xi_c(0)$ (Å)	$d/\xi_c(0)$	λ_I	λ_{II}	λ_{III}
0.00	106	109	150	121	0.59	21.30	8.18	2.61	0.59 (quasi-2D)	2.37 (0D/SW)	0.91 2D
0.10	101	107	178	118	0.6	24.51	9.49	2.58	1.34 (quasi-1D)	0.49 3D	1.09 2D
0.20	93	97	143	106	0.6	40.80	15.80	2.58	0.9 2D	0.34 3D	1.17 2D
0.30	79	87	114	95	0.61	49.83	19.46	2.56	0.81 2D	2.56 (0D/SW)	0.45 3D
0.40	55	76	129	82	0.62	60.35	23.76	2.54	0.15 (quasi-3D)	2.52 (0D/SW)	0.46 3D
0.50	21	52	93	55	0.64	75.53	30.21	2.50	0.65 (quasi-2D)	1.97 (0D/SW)	0.34 3D

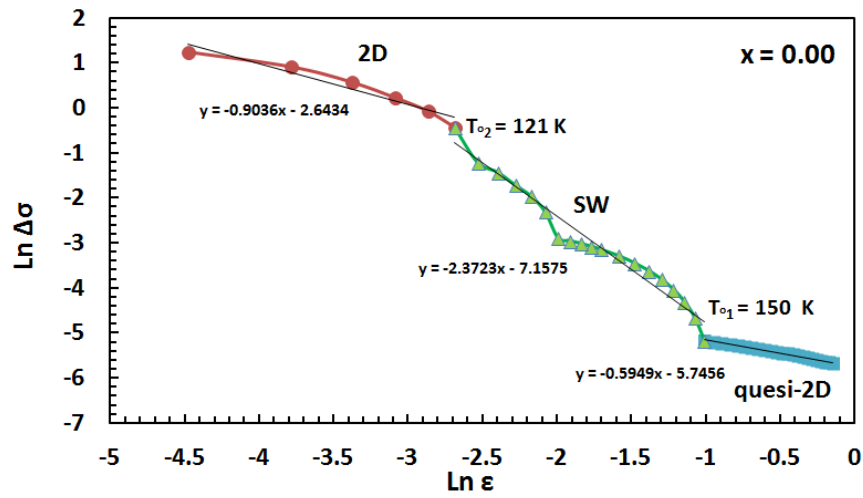


Fig. 3(a). $\ln \Delta\sigma$ against $\ln \epsilon$ for Y doped Bi:2223 samples ($x = 0.00$)

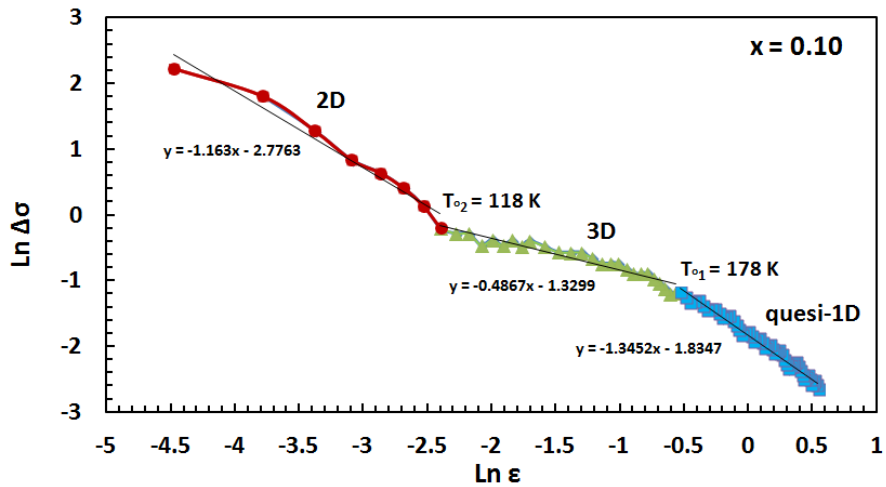


Fig. 3(b). $\ln \Delta\sigma$ against $\ln \epsilon$ for Y doped Bi:2223 samples ($x = 0.10$)

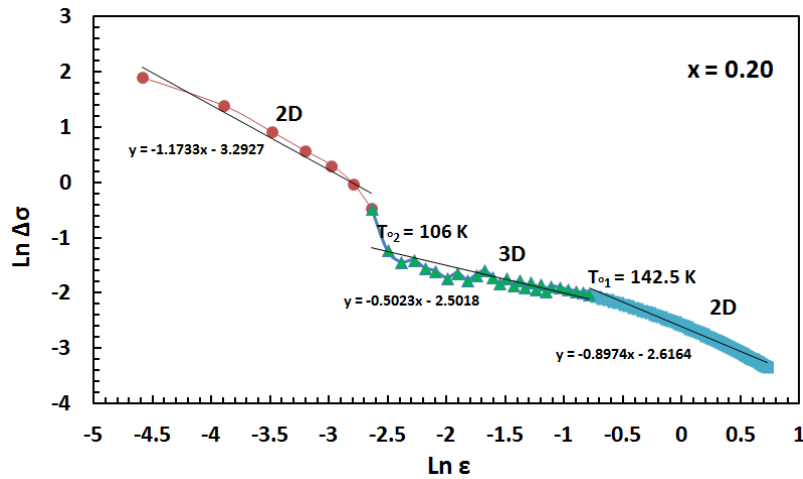


Fig. 3(c). $\ln \Delta\sigma$ against $\ln \epsilon$ for Y doped Bi:2223 samples ($x = 0.20$)

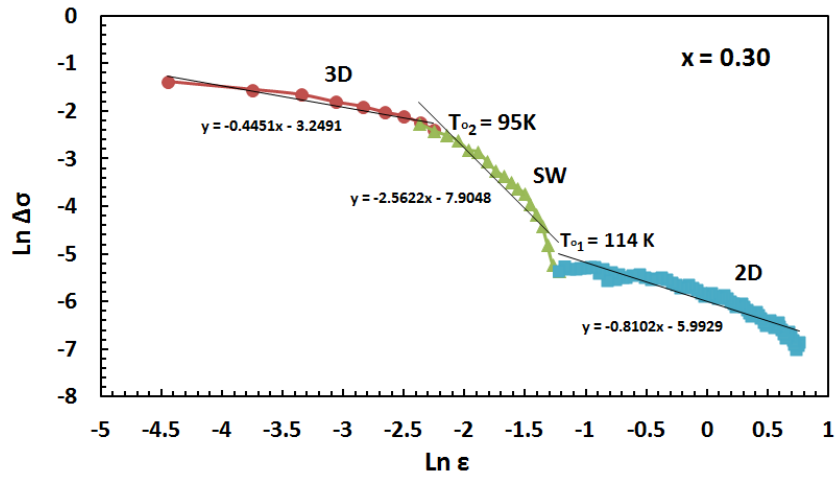


Fig. 3(d). $\ln \Delta\sigma$ against $\ln \epsilon$ for Y doped Bi:2223 samples ($x = 0.30$)

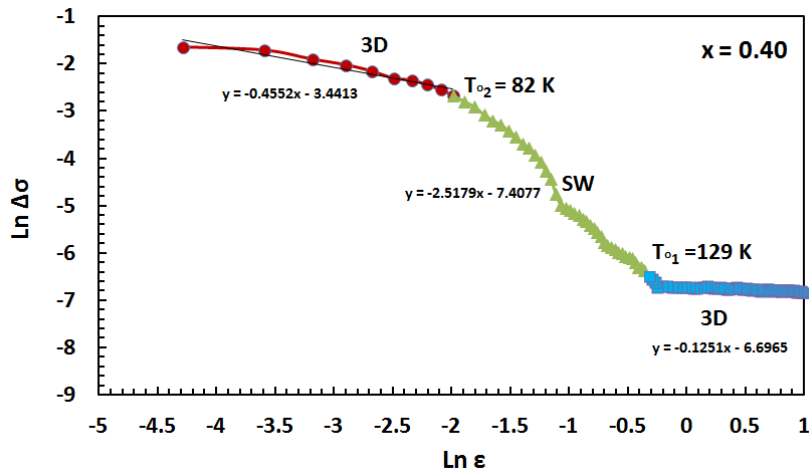


Fig. 3(e). $\ln \Delta\sigma$ against $\ln \epsilon$ for Y doped Bi:2223 samples ($x = 0.40$)

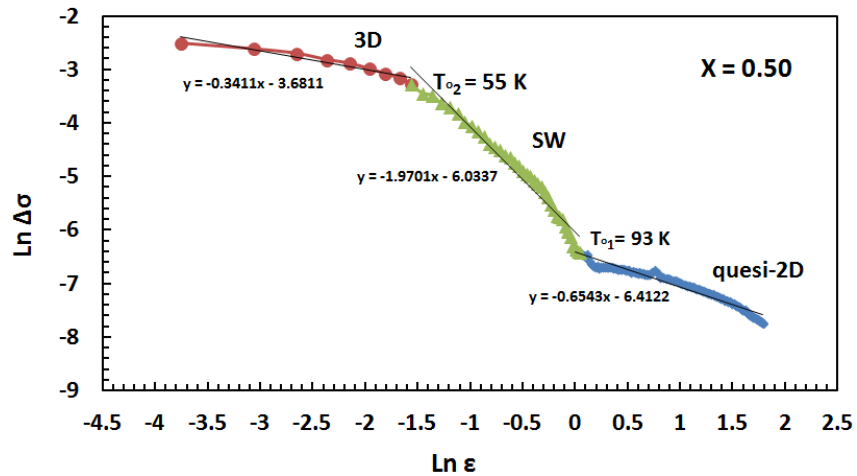


Fig. 3(f). $\ln \Delta\sigma$ against $\ln \epsilon$ for Y doped Bi:2223 samples ($x = 0.50$)

Anyhow, the crossover behavior occurs at a temperature T_0 is given by [38,39];

$$T_0 = T_c^{mf} \exp\left(\frac{2\xi_c(0)}{d}\right)^2 \quad (3)$$

, where $\xi_c(0)$ is given by $\xi_c(0) = \frac{dJ^{\frac{1}{2}}}{2}$ and J is the

interlayer coupling expressed by $J = \ln \frac{T_0}{2T_c^{mf}}$

[40,41]. The average values of interlayer coupling J are calculated in terms of the values of T_{02} and T_c^{mf} , and listed in Table 1. It is found that J slightly increased by increasing x , and their values are between 0.59 and 0.64 for all samples. The samples of $x = 0.00, 0.10$ and 0.20

are 2D nature, and the intersection $A = \frac{e^2}{32\hbar d}$

for 2D. Therefore, d and $\xi_c(0)$ are calculated from the values of A and J , respectively. While the samples of $x = 0.30, 0.40$ and 0.50 are 3D

nature, and the intersection $A = \frac{e^2}{32\hbar \xi_c(0)}$ for

3D. Therefore, $\xi_c(0)$ and d are calculated from the values of A and J , respectively.

Fig. 4 shows the behavior of both d and $\xi_c(0)$ against x , and similar values are listed in Table 2. It is clear that both d and $\xi_c(0)$ are increased as x increases, but the values of d are higher than that of $\xi_c(0)$, indicating the 2D nature of superconductivity, in agreement with the reported data [21-27]. The increase of $\xi_c(0)$ at ($x > 0.20$) indicates that Y substitution shifts the hole carriers from the optimum doped region of the pure sample towards the over doped region [42]. Similar results are obtained by Wen et al. [28] for La: 214 superconductors. They found a drop of the coherence length in the under-doped region followed by an increase in the over-doped beside an increase of hole-concentration. The values of $[d/\xi_c(0)]$ shown in Table 1 are between 2.51 and 2.60 for all samples, which is probably related to a constant values of J as discussed above.

The critical field $H_c(0)$, lower critical field $H_{c1}(0)$, upper critical fields $H_{c2}(0)$ and critical current density at 0 K are estimated by the following relations [42,43-46].

$$H_c(0) = \frac{\phi_0}{2\sqrt{2}\pi\lambda(0)\xi_c(0)};$$

$$H_{c1}(0) = \frac{H_c(0)\ln\kappa}{\sqrt{2}\kappa} \quad (4a)$$

$$H_{c2}(0) = \sqrt{2}\kappa H_c(0);$$

$$J_c(0) = \frac{4\kappa H_{c1}(0)}{3\sqrt{3}\lambda(0)\ln\kappa} \quad (4b)$$

$\phi_0 = 2.07 \times 10^{-15} (T.m^2)$, κ is Ginsberg-Landau parameter of the superconducting system given

by; $\kappa = \frac{\lambda(0)}{\xi_c(0)}$, where $\lambda(0)$ is the London

penetration depth at 0 K, which is about 300 nm for Bi:2223 superconductors [47]. However, the values of κ listed in Table 2 are decreased as x increases up to 0.50. Similar behavior is obtained for the critical values of fields and current as shown as in Fig. 4 (a,b). This behavior may be due to a decrease of grain boundaries resistance and superconducting volume fraction of (Bi, Pb)-2223 single phase as x increases [42,47].

The anisotropy parameter could be obtained using the relation [48];

$$\gamma = \left[\frac{0.71 K_B}{\sqrt{N_G B_c^2(0) \xi_c^3(0)}} \right]^{\frac{1}{2}} \quad (5)$$

K_B is Boltzmann constant and N_G is Ginzberg reduced number given by the relation;

$$N_G = \frac{T_0 - T_c}{T_c} . \quad \text{From the values of}$$

anisotropy, the in-plane coherence length at 0 K, $\xi_{ab}(0)$ could be obtained using the relation,

$$\gamma = \frac{\xi_{ab}(0)}{\xi_c(0)} . \quad \text{It is clear from Table 2 that both } N_G ,$$

γ and ξ_{ab} are generally increased as x increases up to 0.50. Similar behavior between the above parameter and x are also obtained in Figs. 4 and 6.

The Ginzburg number, G_i , defines the order thermal fluctuations in a superconductor is given by [49-50];

$$G_i = \left[\frac{\pi \kappa^2 \xi_0(c) K_B T_c \mu_0}{2 \phi_0^2} \right]^2 \quad (6)$$

where $\mu_0 = 4\pi \times 10^{-7}$ A/m and K_B is Boltzmann constant. The values of G_i are calculated for all samples and shown in Fig. 6, and similar values are listed in Table 2. It is found that the values of G_i are decreased from 5.48×10^{-3} to 0.016×10^{-3} as x increases up to $x = 0.50$. These values are comparable with the reported, $G_i = (10^{-3} - 10^{-4})$ for HTSC, and they are several orders of magnitude larger than 10^{-9} for conventional superconductor. [51-52]. Decreasing the values of G_i support the decrease of critical temperature and also the shift

of order parameter dimensionality from 2D to 3D as x increases.

However, the fluctuation induced excess conductivity study for the x -doped Bi (Pb):2223 phase are considered by the following points; (i) decreasing the T_c^{mf} as well as T_c ; (ii) appearance of three different exponents corresponding to two crossover temperatures; (iii) In the critical field region, the order parameter exponents are (2D) up to $x = 0.20$, but it is changed to (3D) up to $x = 0.50$; (iv) increasing the coherence lengths, inter-plane spacing, interlayer coupling and anisotropy; (v) decreasing the G-L parameter, Ginzburg number, critical magnetic fields and critical current density.

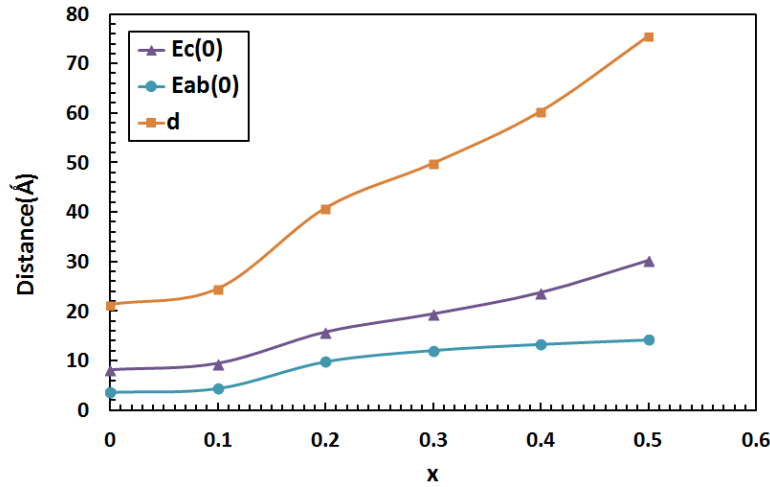


Fig. (4). $d, \xi_{ab}(0)$ and $\xi_c(0)$ versus x for Bi:2223 samples

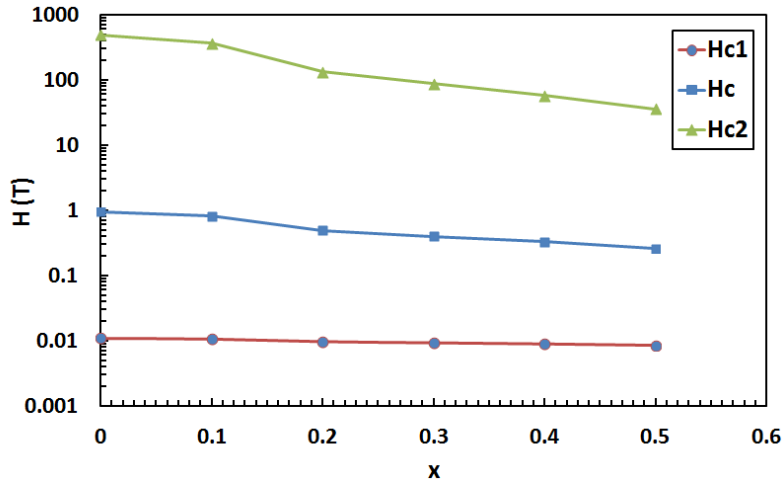


Fig. 5(a). Critical magnetic fields versus x for Bi:2223 samples

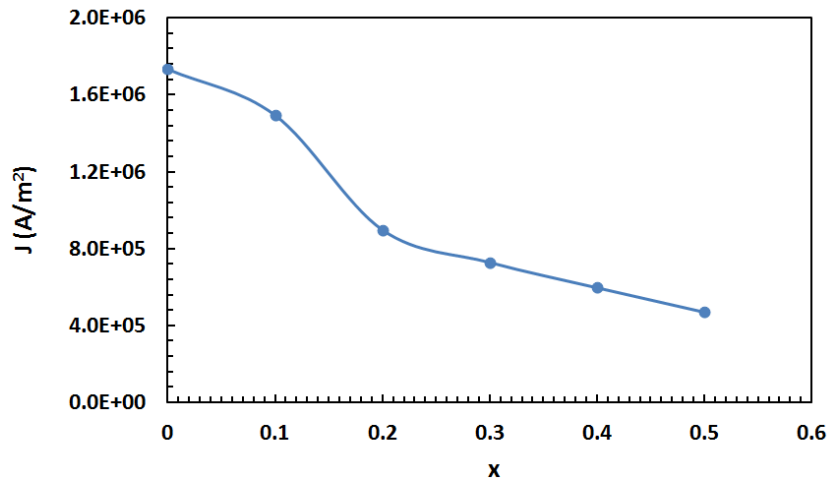


Fig. 5(b). Critical current density versus x for Bi:2223 samples

Table 2. H_c , H_{c1} , H_{c2} , $J_c(0)$, G_i , N_G , γ and $\xi_{ab}(0)$ for Y doped Bi:2223 samples

X	K	H_c (T)	H_{c1} (T)	H_{c2} (T)	J_c (A/m ²)	G_i	N_G	γ	ξ_{ab} (Å)
0.00	366.748	0.95	0.0109	490.94	17.3×10^5	5.48×10^{-3}	0.14	0.44	3.60
0.10	316.122	0.82	0.0106	364.76	14.9×10^5	3.70×10^{-3}	0.17	0.46	4.37
0.20	189.873	0.49	0.0096	131.59	8.97×10^5	1.13×10^{-3}	0.14	0.62	9.80
0.30	154.162	0.40	0.0093	86.75	7.28×10^5	0.54×10^{-3}	0.20	0.62	12.07
0.40	126.263	0.33	0.0089	58.19	5.96×10^5	0.18×10^{-3}	0.49	0.56	13.31
0.50	99.3049	0.26	0.0085	35.99	4.69×10^5	0.016×10^{-3}	1.60	0.47	14.20

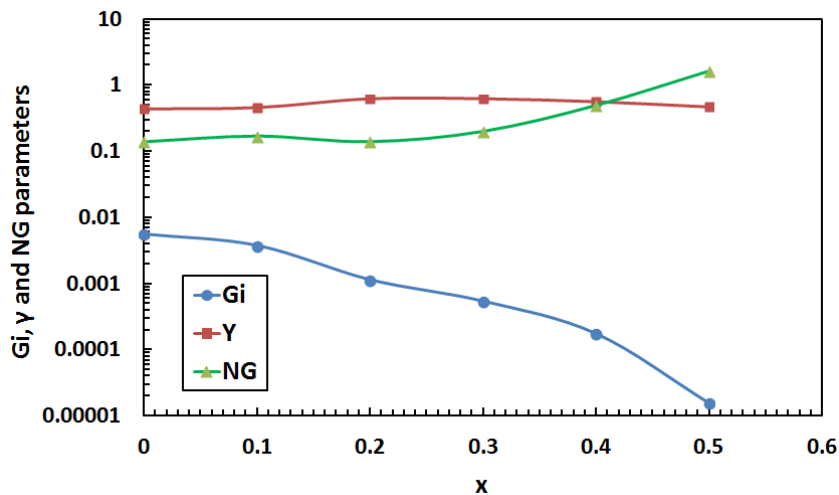


Fig. (6). G_i , γ and N_G versus Y content for Bi:2223 samples

This is due to some reasons such as; decreasing c-lattice parameter by Y substitution at Ca at the same 8-fold co-ordination; increasing the hole carriers concentration per Cu ion in the superconducting state as a result of more positive charges transferred to the Cu-O layer;

the excess oxygen arising from the replacement of 2CaO by one Y_2O_3 molecule; increasing both coherence lengths and anisotropy. The consistency of these points gives a fair degree of certainty to appearance the fluctuation induced

excess conductivity of Y substitution in Bi (Pb):2223 system.

4. CONCLUSION

Fluctuation induced excess conductivity in Y doped Bi: 2223 is reported. We have shown three different values of the order parameter exponents corresponding to two crossover temperatures due to shifting the order parameter dimensionality against a decrease of temperature. In the critical field region, the order parameter exponents are two dimensional (2D) as x increases up to 0.20, but it is changed from 2D to three dimensional (3D) with further increase of x up to 0.50. While, the order parameter exponents are fluctuated between zero dimensional/ short wave fluctuation (0D/SW), quasi-2D, quasi-1D and 3D in the normal and mean field regions. The coherence lengths, inter-plane spacing, interlayer coupling and anisotropy are generally increased by increasing x up to 0.50, whereas G-L parameter, Ginzberg number, critical magnetic fields and critical current density are decreased. The possible reasons for the above findings are also mentioned.

COMPETING INTERESTS

Authors have declared that no competing interests exist.

REFERENCES

1. Biju A. Improved superconducting properties by La addition in (Bi, Pb)-2212 bulk superconductor. *J. Alloys Compd.* 2007;431:49-55.
2. Sedky A, Al-Battat W. Effect of Y substitution at Ca site on structural and superconducting properties of Bi:2212 superconductor. *Physica B.* 2013;410:227-232.
3. Jr CP. Poole, Farach HA, Cheswick RJ, Prozorov R, *Superconductivity*, 2nd ed. Amsterdam: Elsevier; 2007.
4. Terzioglu C, Aydin H, Ozturk O, Bekiroglu E, Belenli I. The influence of Gd addition on microstructure and transport properties of Bi-2223. *Physica B.* 2008;403:3354-3359.
5. Gul IH, Rehman MA, Ali M, Maqsood A. Effect of vanadium and barium on the Bi-based (2223) *Physica C.* 2005;432:71-80.
6. Torrance JB, Bezingue A, Nazzal AI, Parkin SSP. Disappearance of high temperature superconductivity induced by high carrier concentrations. *Physica C.* 1989;(162–164):291-295.
7. Torrance JB, Tokura Y, Nazzal AI, Bezingue A, Huang TC, Parkin SSP. Anomalous disappearance of high- T_c superconductivity at high hole concentration in metallic $\text{La}_{2-x}\text{Sr}_x\text{CuO}_4$. *Phys. Rev. Lett.* 1988;61: 1127-1130.
8. Mandal P, Poddar A, Ghosh B, Choudhury P. Variation of T_c and transport properties with carrier concentration in Y-and Pb-doped Bi-based superconductors. *Phys. Rev. B* 43. 1991;16:13102-13111.
9. Narlikar AV, Rao CV, Agarwal SK. *Studies of high temperature super-conductors*, Nova, New York. 1989;1:341.
10. Cimberle MR, Ferdeghini C, Giannini E, Marre D, Putti M, Siri A, Federici F, Varlomov A. Crossover between Aslamazov-Larkin and short-wavelength fluctuation regimes in high-temperature-superconductor conductivity experiments. *Phys. Rev. B.* 1997;55:14745-14748.
11. Harabor A, Harabor NA, Deletter M. Short-wavelength fluctuation regime in paraconductivity of bulk monophas (Bi, Pb)-2223 superconductor system. *J. Optoelectron. Adv. M.* 2006;8:1072-1076.
12. Aswal K, Singh A, Sen S, Kaur M, Viswandham CS, Goswami GL, Gupta SK. Effect of grain boundaries on paraconductivity of $\text{YBa}_2\text{Cu}_3\text{O}_x$. *J. Phys. Chem. Solids.* 2002;63:1797-1803.
13. Sahoo M, Behera D. SCOPF analysis of $\text{YBa}_2\text{Cu}_3\text{O}_{7-\delta} + x\text{Cr}_2\text{O}_3$ superconductor composite. *J. Phys. Chem. Solids.* 2013;74: 950-956.
14. Esmaeili A, Sedghi H. Excess-conductivity of $\text{Nd}_{0.1}\text{Y}_{0.9}\text{Ba}_2\text{Cu}_3\text{O}_{7-\delta}$ and $\text{Ca}_{0.1}\text{Y}_{0.9}\text{Ba}_2\text{Cu}_3\text{O}_{7-\delta}$ superconductors. A quantitative comparison between results of aliovalent and isovalent substitutions in Y-site. *J. Alloys Compd.* 2012;537:29-34.
15. Ibrahim EMM, Saleh SA. Influence of sintering temperature on excess conductivity in Bi-2223 superconductors. *Supercond. Sci. Technol.* 2007;20:672-675.
16. Maki K, Thompson RS. Fluctuation conductivity of high- T_c superconductors. *Phys. Rev. B.* 1988;39:2767-2770.
17. Vidal F, Veira JA, Maja J, Ponte JJ, Alvarado FG, Mordan E, Amador J, Cascales C. Excess electrical conductivity

- in polycrystalline Bi-Ca-Sr-Cu-O compounds and thermodynamic fluctuations of the amplitude of the superconducting order parameter. *Physica C*. 1988;156:807-816.
18. Ben Azzouz F, Annabi M, Zouaoui M, Ben Salem M. Effects of Al₂O₃ nanometer particles addition on the fluctuation conductivity in (Bi, Pb)-2223 superconductors. *Phys. Stat. Sol. (c)*. 2006;9:2978-2981.
 19. Baraduc V, Pagnon A, Buzdin J. Henry and C. Ayache, Specific paraconductivity along the c-axis in YBa₂Cu₃O₇. *Phys. Lett. A*. 1992;166:267-272.
 20. Mohapatra UK, Biswal R, Behera D, Mishra N. Fluctuation conductivity and inhomogeneity in granular YBa₂Cu₃O_{7-y}/Ag composite thick films. *Supercond. Sci. Technol*. 2006;19:635-640.
 21. Jurelo AR, Kunzler JV, Schaf J, Pureur P. Fluctuation conductivity and microscopic granularity in Bi-based high temperature superconductors. *Phys. Rev. B*. 1997;56:14815-14821.
 22. Vidal F, Veira JA, Maza J, Ponte JJ, Alvarado F, Moran E, Amador J, Cascales C, Castro A, Casais MT, Rasines I. Excess electrical conductivity in polycrystalline Bi-Ca-Sr-Cu-O compounds and thermodynamic fluctuations of the amplitude of the superconducting order parameter. *Physica C*. 1988;156:807-816.
 23. Schnelle W, Braun E, Broicher H, Weiss H, Geus H, Ruppel S, Galfy M, Braunisch W, Waldorf A, Seidler F, Wohlleben. Superconducting fluctuation in Bi₂Sr₂Ca₂Cu₃O_x. *Physica C*. 1989;161:123-135.
 24. Balestrino G, Nigro A, Vaglio R. Thermodynamic fluctuations in the 110-K Bi-Sr-Ca-Cu-O superconductor: Evidence for two-dimensional behavior. *Phys. Rev. B*. 1989;39:12264-12266.
 25. Veira JA, Vidal F. Scattering of normal excitations by superconducting fluctuations in single-crystal and granular copper oxide superconductors. *Phys. Rev. B*. 1990;42:8748-8751.
 26. Khalil SM. Effect of Cd addition on superconducting fluctuations and mechanical properties of Bi_{1.82}Pb_{0.36}Sr₂Ca₂Cd_xCu₃O_y System. *J. Low Temp. Phys*. 2006;143(1-2):31-44.
 27. Mishra DR, Gd-substituted Bi-2223 superconductor. *Pramana. J. Physics*. 2008;70(3):535-541.
 28. Sedky A. The impact of Y substitution on the 110 K high T_c phase in a Bi (Pb):2223 superconductor. *J. Phys. and Chemistry of Solids*. 2009;70:483-488.
 29. Rojas Sarmiento MP, Uribe Laverde MA, Vera López E, Landineza DA, Roa-Rojas J. Conductivity fluctuation and superconducting parameters of the YBa₂Cu_{3-x}(PO₄)_xO_{7-δ} material. *Physica B*. 2007;398:360-363.
 30. Buckley RG, Tallon JL, Pooke DM, Presland MR. Calcium-substituted superconducting RBa₂Cu₄O₈ with T_c~ 90K prepared at one atmosphere. *Physica C*. 1990;165:391-396.
 31. Das A, Suryanarayanan R. Remarkable influence of heat treatment on the structural and superconducting properties of Y_{1-x}Pr_xSrBaCu₃O_{6+z}. *J. Phys. I France*. 1995;5:623-630.
 32. Reggiani L, Vaglio R, Varlamo AA. Fluctuation conductivity of layered high-T_c superconductors: A theoretical analysis of recent experiments. *Phys. Rev. B*. 1991;44:9541-9546.
 33. Lawrence WE, Doniach S, in Proc. 12th Conf. Low-Temp. Phys., p. 361, Tokyo; 1970.
 34. Ben Azzouz F, Zouaoui M, Annabi M, Ben Salem M. Fluctuation conductivity analysis on the Bi-based superconductors processed under same conditions. *Phys. Stat. Sol. (c)*. 2006;3(9):3048-3051.
 35. Lobb CJ. Critical fluctuations in high-T_c superconductors. *Phys. Rev. B*. 1987;36:3930-3932.
 36. Hohenberg PC, Halperin BI. Theory of dynamic critical phenomena. *Rev. Mod. Phys*. 1977;49:435-479. Anderson W, Zou Z. "Normal" Tunneling and "Normal" Transport: Diagnostics for the Resonating-Valence-Bond State. *Phys. Rev. Lett*. 1988;60:132-135.
 37. Roumié M, Abdeen W, Awad R, Korek M, Hassan I, Mawassi R. Excess conductivity analysis of Bi_{1.8}Pb_{0.4}Sr₂Ca₂Cu₃O_{10+δ} added with Nano-ZnO and Nano-Fe₂O₃. *J. Low Temp. Phys*. 2014;174:45-63.
 38. Aslamazov LG, Larkin AI. The influence of fluctuation pairing of electrons on the conductivity of normal metal. *Phys. Lett. A*. 1968;26:238-239.
 39. Lawrence WE, Doniach S. Proc. 12th Int. Conf. Low Temp. Phys. Kyoto (Edited by E. Kanada), Keigaku, Tokyo. 1971;361.
 40. Gosh AK, Bandyopadhyay SK, Basu AN. Generalization of fluctuation induced

- conductivity in polycrystalline $Y_{1-x}Ca_xBa_2Cu_3O_y$ and $Bi_2Sr_2Ca_1Cu_2O_{8+\delta}$. Superconductors. J. Appl. Phys. 1999;86: 3247-3252.
41. Ghosh AK, Bandyopadhyay SK, Barat P, PintuSen, Basu AN. Fluctuation-induced conductivity of polycrystalline $Y_{1-x}Ca_xBa_2Cu_3O_{7-\delta}$ superconductors. Physica C. 1996;264:255-260.
 42. Abou-Aly AI, Awad R, Kamal M, Anas M, Excess conductivity analysis of $(Cu_{0.5}Ti_{0.5})$ -1223 substituted by Pr and La. J. Low Temp Phys. 2011;163:184-202.
 43. Wen HH, Yang HP, Li SL, Zeng XH, Soukiassian AA, Si WD. Hole doping dependence of the coherence length in $La_{2-x}Sr_xCuO_4$ thin films .Europhys. Lett. 2003;64:790-796.
 44. Poole PC, Farach AH, Creswick JR, Prozorov R. Superconductivity, 2nd edn. (Academic Press, Elsevier, San Diego, 2007).
 45. AbouAly AI, Ibrahim IH, Awad R, El-Harizy A, Khalaf A. Stabilization of TI-1223 Phase by Arsenic SubstitutionJ.Supercond. Nov. Magn. 2010;23(7):1325-1332.
 46. Abou-Aly AI, Awad R, Ibrahim IH, Abdeen W. Excess conductivity analysis for $Tl_{0.8}Hg_{0.2}Ba_2Ca_2Cu_3O_{9-\delta}$ substituted by Sm and Yb. Solid State Commun. 2009;149: 281-285.
 47. Sedky A. On the study of Müllers model in high-temperature superconductors J. Magnetism and Mag. Materials. 2004;277: 293-297.
 48. Petrovie A, Fasano Y, Lortz R, Decrouc M, Potel M, Chevrel R, Fischer O. Unconventional resistive transitions in the extreme type-II superconductor $Tl_2Mo_6Se_6$. Physica C. 2007;(460-462):702-703.
 49. Jaroszynski J, Riggs SC, Hunte F, Gurevich A, Larbalestier DC, Boebinger GS, Balakirev FF, Migliori A, et al. Comparative high-field magnetotransport of the oxypnictide superconductors $RFeAsO_{1-x}F_x$ (R=La, Nd) and $SmFeAsO_{1-\delta}$. Phys. Rev. B. 2008;78: 064511-064515.
 50. Mun MO, Lee SI, Lee WC. Fluctuation magneto conductance in RNi_2B_2C (R=Y and Lu) single crystals. Phys. Rev. B. 1997;56:14668-14670.
 51. Pribulova Z, Klein T, Kacmarcik J, Marcenat C, Konczykowski M, Bud'ko SL, Tillman M, Canfield PC. Upper and lower critical magnetic fields of superconducting $NdFeAsO_{1-x}F_x$ single crystals studied by Hall-probe magnetization and specific heat.Phys. Rev. B. 2009;79:020508-020511.
 52. Kim S, Choi C, Jung M, Yoon J, Jo Y, Wang X, Chen X, Wang XL, Lee S, Choi K, Fluctuation conductivity of single-crystalline $BaFe_{1.8}Co_{0.2}As_2$ in the critical region..Journal of Applied Physics. 2010; 108(6):063916.

© 2017 Sedky et al.; This is an Open Access article distributed under the terms of the Creative Commons Attribution License (<http://creativecommons.org/licenses/by/4.0>), which permits unrestricted use, distribution, and reproduction in any medium, provided the original work is properly cited.

Peer-review history:
The peer review history for this paper can be accessed here:
<http://sciencedomain.org/review-history/21326>